Supplementary information for

Processes driving the regional sensitivities of summertime $PM_{2.5}$ to temperature across the US: New insights from model simulations

Lifei Yin et al.

Correspondence to: Pengfei Liu (pengfei.liu@eas.gatech.edu)

Supplementary Figure 1. The categorization of four subregions of the contiguous United States used in this study.

Supplementary Figure 2. Same as Figure 1 a1-a5 in the main text but displaying only temperature sensitivities that are statistically significant ($p < 0.05$).

Supplementary Figure 3. Spatial distribution of average summer concentrations of $PM_{2.5}$ and its species derived from ground-based observations and four GEOS-Chem simulation cases. Panels (a1–f1) show the concentrations of $PM_{2.5}$ (a1–a5), organic aerosol (OA) (b1–b5), sulfate (c1–c5), nitrate (d1–d5), ammonium (e1–e5), and black carbon (BC) (f1–f5) for BASE case (2000-2017 average), MOD case (2000-2022 average), MOD_BC case (2000-2022 average), and SIM_BC case (2000-2017 average). Detailed descriptions of the GEOS-Chem simulation cases are provided in Table 1 of the main text.

Supplementary Figure 4. Time series of regional average concentrations derived from ground-based observations, machine-learning-modeled data, and four GEOS-Chem simulation cases. Panels (a1–f1) show the concentrations of $PM_{2.5}$ (a1–a5), organic aerosol (OA) (b1–b5), sulfate (c1–c5), nitrate (d1–d5), ammonium (e1–e5), and black carbon (BC) (f1–f5) for the contiguous US (a1–f1), Southeast US (a2–f2), Northeast US (a3–f3), West US (a4–f4), and Central US (a5–f5).

Supplementary Figure 5. NH_3 emissions during summer months (June, July, August) from the NEI 2011 inventory and the NEI 2016 inventory for the contiguous United States (a) and the Southeast US (b).

Supplementary Figure 6 Sensitivities of surface concentration to summer mean temperature anomalies for five major components of $PM_{2.5}$ derived from four GEOS-Chem cases and ground-based observations from 2000-2016. Triangle markers represent fitted slopes (sensitivities) with $p<0.05$. a-e, temperature sensitivity of summertime organic aerosols (OA) (a1-a4), sulfate (b1-b4), ammonium (c1-c4), nitrate (d1-d4), and elemental carbon (EC) (e1-e4) simulated by BASE case, MOD case, MOD_BC case, and SIM_BC case. Please refer to Table 1 in the main text for details on the GEOS-Chem cases.

Supplementary Figure 7 Regional sensitivities of surface concentration to summer mean temperature anomalies five major components of $PM_{2.5}$ derived from four GEOS-Chem cases and ground-based observations from 2000-2016. a-e, temperature sensitivity of organic aerosols (OA), sulfate, ammonium, nitrate, and elemental carbon (EC). For each region, the bars (from left to right) represent results from observations (OBS), BASE case, MOD case, MOD_BC case, and SIM_BC case. Detailed descriptions of the GEOS-Chem simulation cases are provided in Table 1 of the main text.

Supplementary Figure 8. Daytime slopes of monthly mean cloud fractions in the lower troposphere (> 680 hPa) versus surface air temperature over land for June–July–August during 2000–2022, based on MERRA2 meteorology. White areas indicate slopes that are not statistically significant at the 0.05 level.

Supplementary Figure 9. Annual scaling factors for SO_2 emissions from energy generation units, derived from the NEI inventory and raw CAMD data.

Supplementary Figure 10. CAMD-derived scaling factors for SO_2 emissions (a) and NO_x emissions (b) from energy generation units during summer months.

Supplementary Figure 11. Coefficient of determination (r^2) and root-mean-square error (RMSE) between observations and four GEOS-Chem cases for $PM_{2.5}$ and its five major components. Panels (a1–f1) show the r^2 values for $PM_{2.5}$, organic aerosols (OA), sulfate, ammonium, nitrate, and black carbon (BC), respectively. Panels (a1–f1) show the corresponding RMSE values for the same species.

Supplementary Figure 12. Same as Figure 2 in the main text, but for ammonium, nitrate, and black carbon (BC).

Supplementary Figure 13. Regional-aggregated temperature sensitivity of three major organic aerosol (OA) species from four GEOS-Chem cases. Panels a1-a5 shows the temperature sensitivity of primary OA for the contiguous US (a1), the Southeast US (a2), the Northeast US (a3), the West US (a4), and the Central US (a5); Panels b1-b5 shows the temperature sensitivity of aqueous-phase formed isoprene OA (ISOAAQ) for each region; Panels c1-c5 shows the temperature sensitivity of monoterpene SOA (TSOA) for each region. The SIM_BC case reports total SOA concentrations as a single variable SOAS, which is shown with ISOAAQ in panels b1-b5.

Supplementary Figure 14. Budget diagnostic for aqueous-phase-formed isoprene SOA (ISOAAQ) simulated by the MOD case and the temperature sensitivity of each process. Panels (a1–d1) show the budget diagnostic for transport (a1), mixing (b1), wet deposition (c1), and convention (d1) process and the corresponding temperature sensitivity (a2-d2).

Supplementary Figure 15. Same as Supplementary Figure 14 but for sulfate budget diagnostic.

Supplementary Figure 16. Time series for budget diagnostic and efficiency of driving processes of ISOAAQ concentration. Panels a1-a5 shows the time series for budget diagnostic for the

contiguous US (a1), the Southeast US (a2), the Northeast US (a3), the West US (a4), and the Central US (a5); Panels b1-b5 shows the time series for removal efficiency for each region.

Supplementary Figure 17. Same as Figure 16 but for sulfate budget diagnostic.

Supplementary Figure 18. Same as Figure 5 in the main text but for primary organic aerosol (POA) and secondary organic aerosol formed from monoterpene oxidation (TSOA).

Supplementary Figure 19. Production rate (a1-a3) and corresponding temperature sensitivity (b1-b3) of three major sulfate production processes. Panels c1-c5 shows the time series for temperature sensitivity of each pathway for the contiguous US (a1), the Southeast US (a2), the Northeast US (a3), the West US (a4), and the Central US (a5).

Supplementary Figure 20. Contributions from isoprene-mediated and sulfate-mediated processes to the overall temperature sensitivity of isoprene SOA (ISOAAQ). The shading areas represent 95% confidence interval. Panels a1-a5 show the time series of isoprene-mediated process breakdown for the contiguous US (a1), Southeast US (a2), Northeast US (a3), West US (a4), and Central US (a5); Panels b1-b5 show the time series of sulfate-mediated process breakdown for each region. Please refer to Eq. (1) in the main text for detailed expression.

Supplementary Figure 21. Same as Supplementary Figure 20 but for sulfate. Please refer to Eq. (2) in the main text for detailed expression.

Supplementary Figure 22. Same as Supplementary Figure 20 but for monoterpene SOA (TSOA). Please refer to Eq. (3) in the main text for detailed expression.

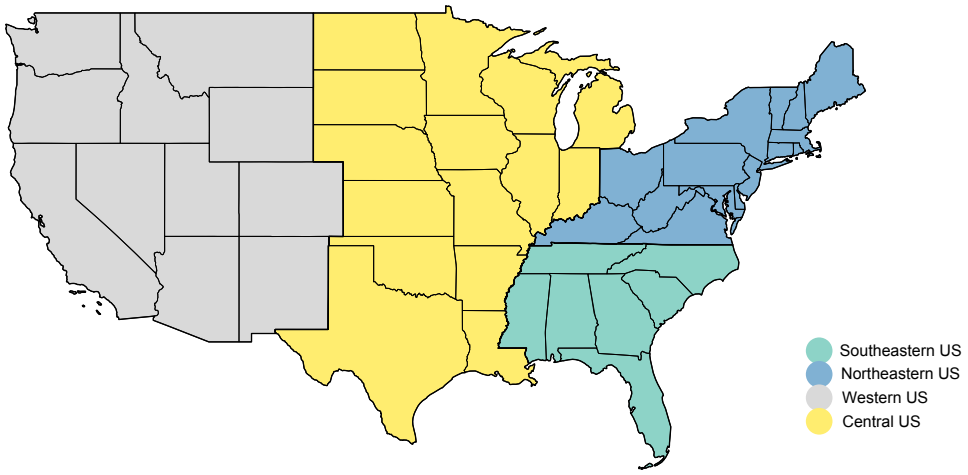

Supplementary Figure 1. The categorization of four subregions of the contiguous United States used in this study.

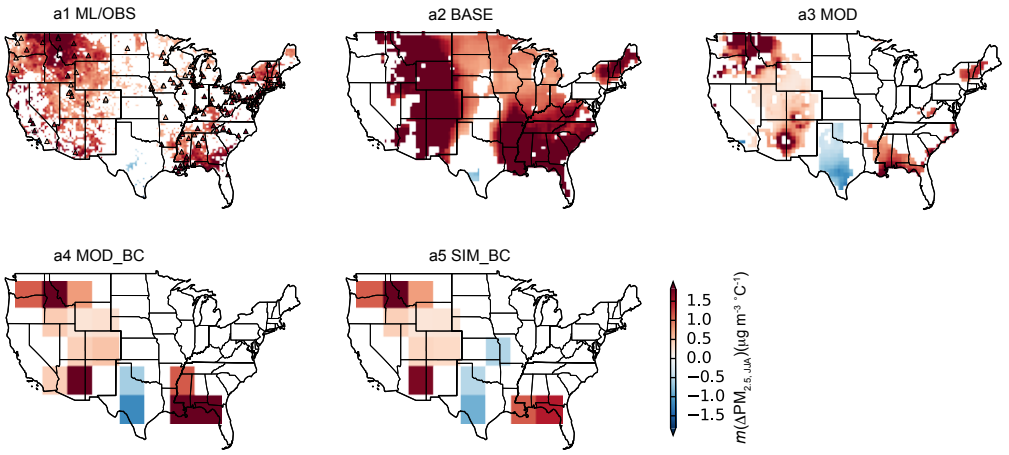

Supplementary Figure 2. Same as Figure 1 a1-a5 in the main text but displaying only temperature sensitivities that are statistically significant ($p < 0.05$).

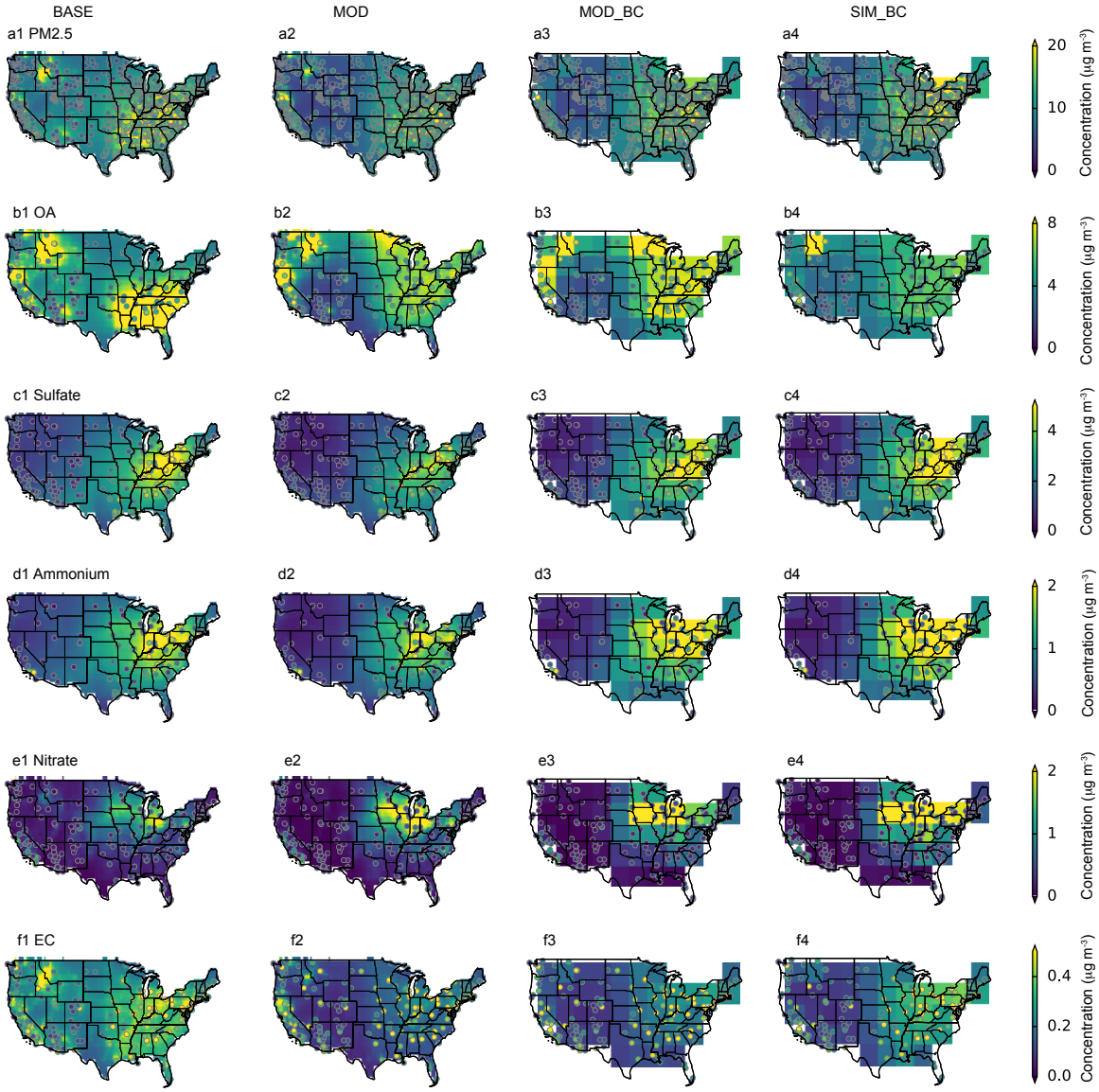

Supplementary Figure 3. Spatial distribution of average summer concentrations of $PM_{2.5}$ and its species derived from ground-based observations and four GEOS-Chem simulation cases. Panels (a1–f1) show the concentrations of $PM_{2.5}$ (a1–a5), organic aerosol (OA) (b1–b5), sulfate (c1–c5), nitrate (d1–d5), ammonium (e1–e5), and black carbon (BC) (f1–f5) for BASE case (2000-2017 average), MOD case (2000-2022 average), MOD_BC case (2000-2022 average), and SIM_BC case (2000-2017 average). Detailed descriptions of the GEOS-Chem simulation cases are provided in Table 1 of the main text.

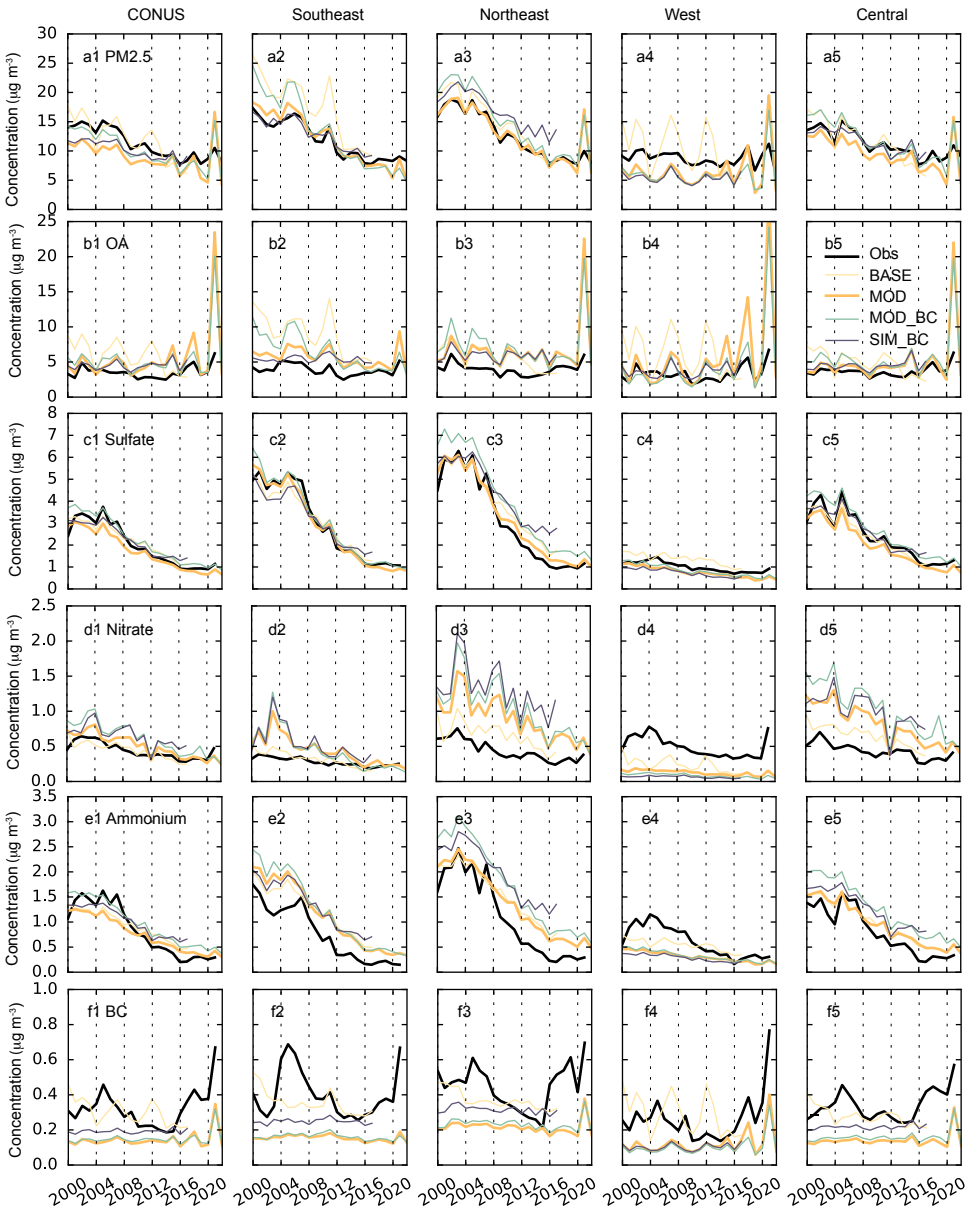

Supplementary Figure 4. Time series of regional average concentrations derived from ground-based observations, machine-learning-modeled data, and four GEOS-Chem simulation cases. Panels (a1–f1) show the concentrations of $PM_{2.5}$ (a1–a5), organic aerosol (OA) (b1–b5), sulfate (c1–c5), nitrate (d1–d5), ammonium (e1–e5), and black carbon (BC) (f1–f5) for the contiguous US (a1–f1), Southeast US (a2–f2), Northeast US (a3–f3), West US (a4–f4), and Central US (a5–f5).

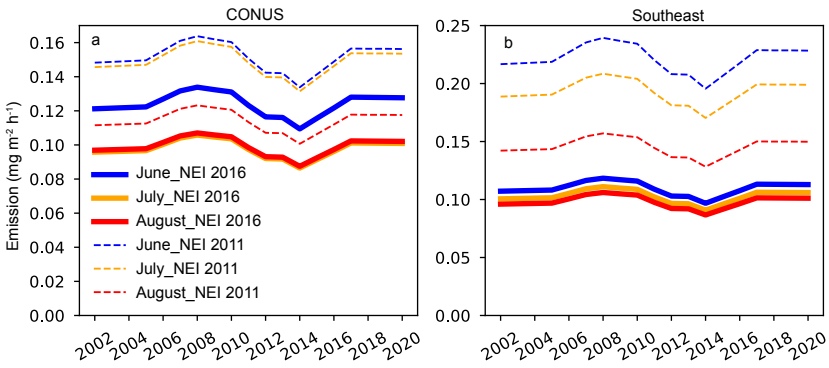

Supplementary Figure 5. NH_3 emissions during summer months (June, July, August) from the NEI 2011 inventory and the NEI 2016 inventory for the contiguous United States (a) and the Southeast US (b).

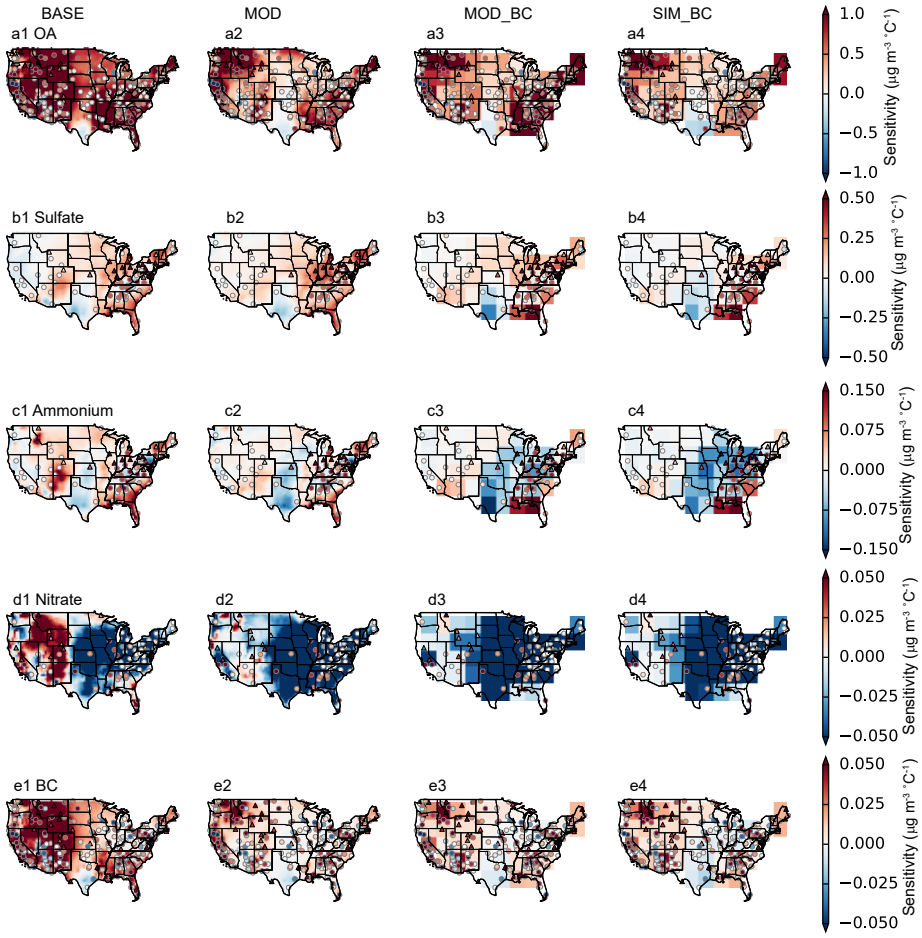

Supplementary Figure 6 Sensitivities of surface concentration to summer mean temperature anomalies for five major components of $PM_{2.5}$ derived from four GEOS-Chem cases and ground-based observations. Triangle markers represent fitted slopes (sensitivities) with $p < 0.05$. a-e, temperature sensitivity of summertime organic aerosols (OA) (a1-a4), sulfate (b1-b4), ammonium (c1-c4), nitrate (d1-d4), and elemental carbon (EC) (e1-e4) simulated by BASE case, MOD case, MOD_BC case, and SIM_BC case. Please refer to Table 1 in the main text for details on the GEOS-Chem cases.

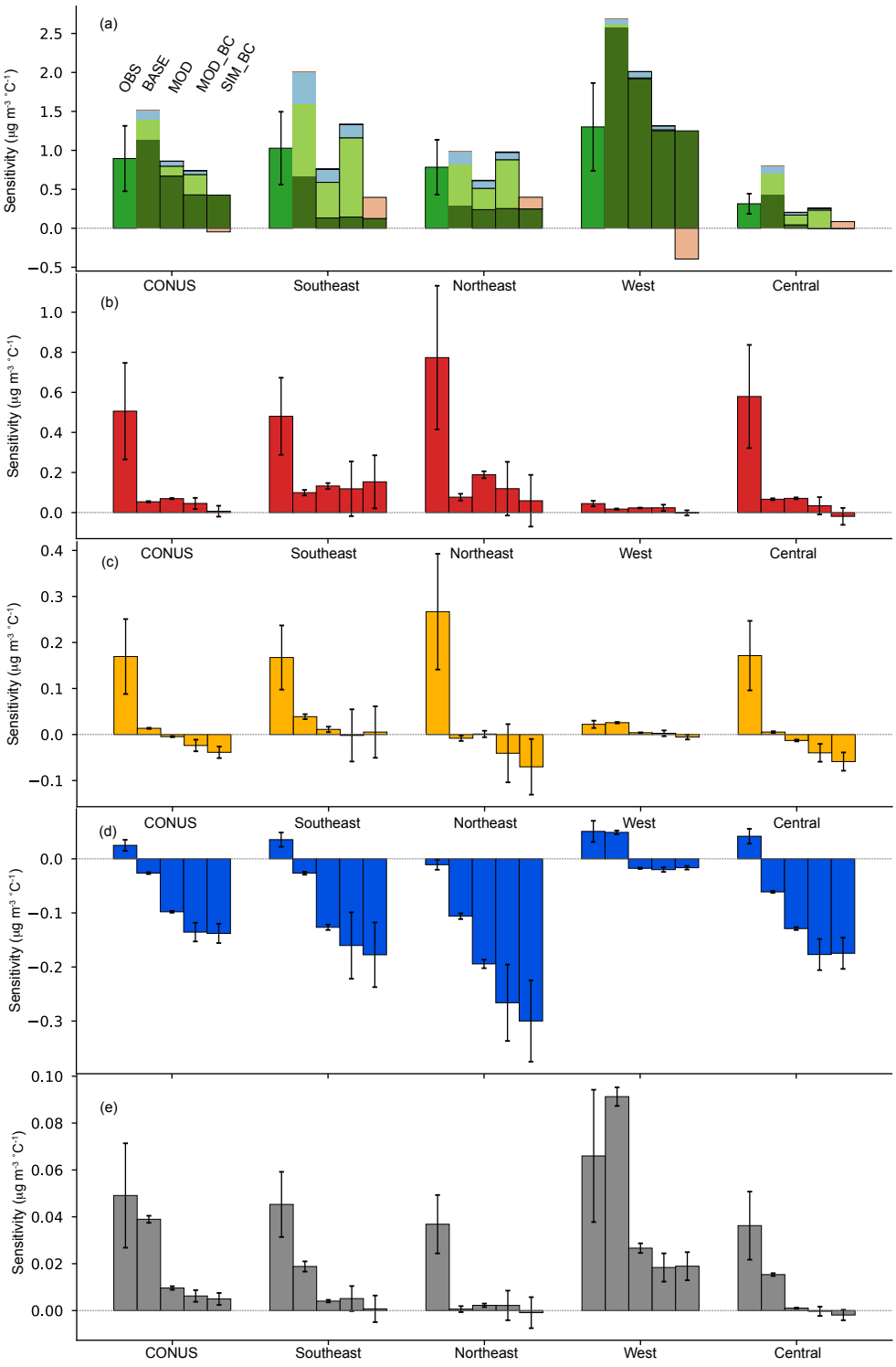

Supplementary Figure 7 Regional sensitivities of surface concentration to summer mean temperature anomalies five major components of $PM_{2.5}$ derived from four GEOS-Chem cases and ground-based observations from 2000-2016. a-e, temperature sensitivity of organic aerosols (OA), sulfate, ammonium, nitrate, and elemental carbon (EC). For each region, the bars (from left to right) represent results from observations (OBS), BASE case, MOD case, MOD_BC case, and SIM_BC case. Detailed descriptions of the GEOS-Chem simulation cases are provided in Table 1 of the main text.

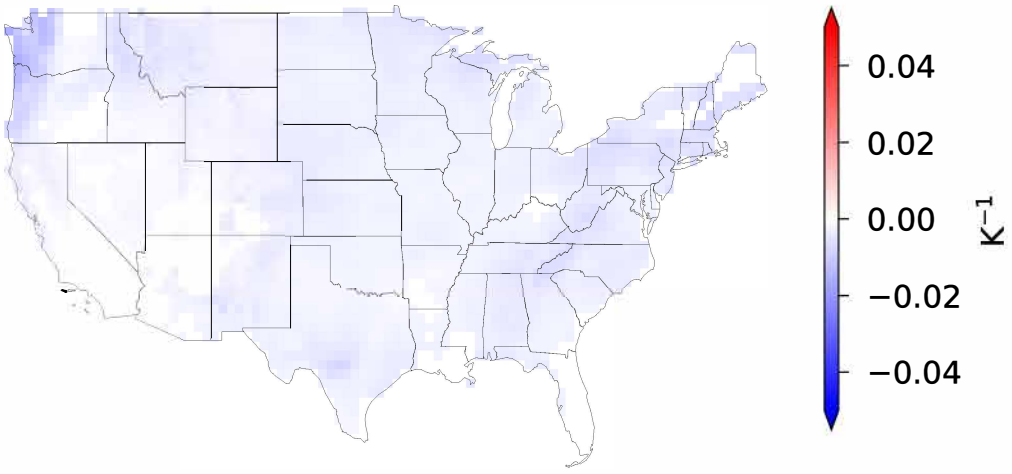

Supplementary Figure 8. Daytime slopes of monthly mean cloud fractions in the lower troposphere (> 680 hPa) versus surface air temperature over land for June–July–August during 2000–2022, based on MERRA2 meteorology. White areas indicate slopes that are not statistically significant at the 0.05 level.

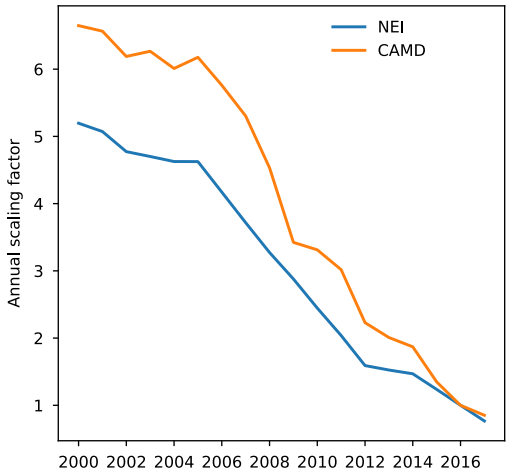

Supplementary Figure 9. Annual scaling factors for SO_2 emissions from energy generation units, derived from the NEI inventory and raw CAMD data.

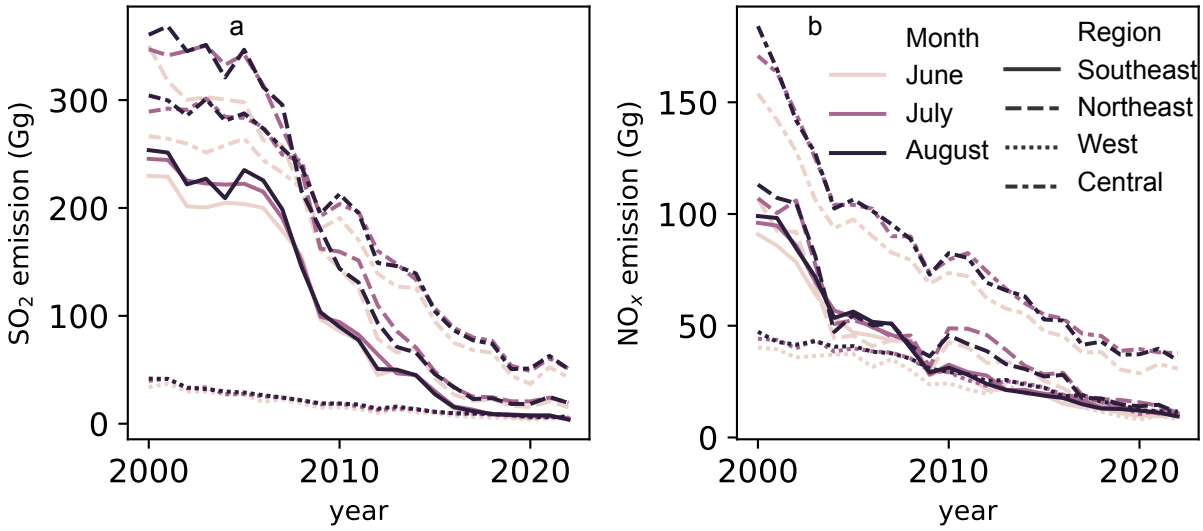

Supplementary Figure 10. CAMD-derived scaling factors for SO_2 emissions (a) and NO_x emissions (b) from energy generation units during summer months.

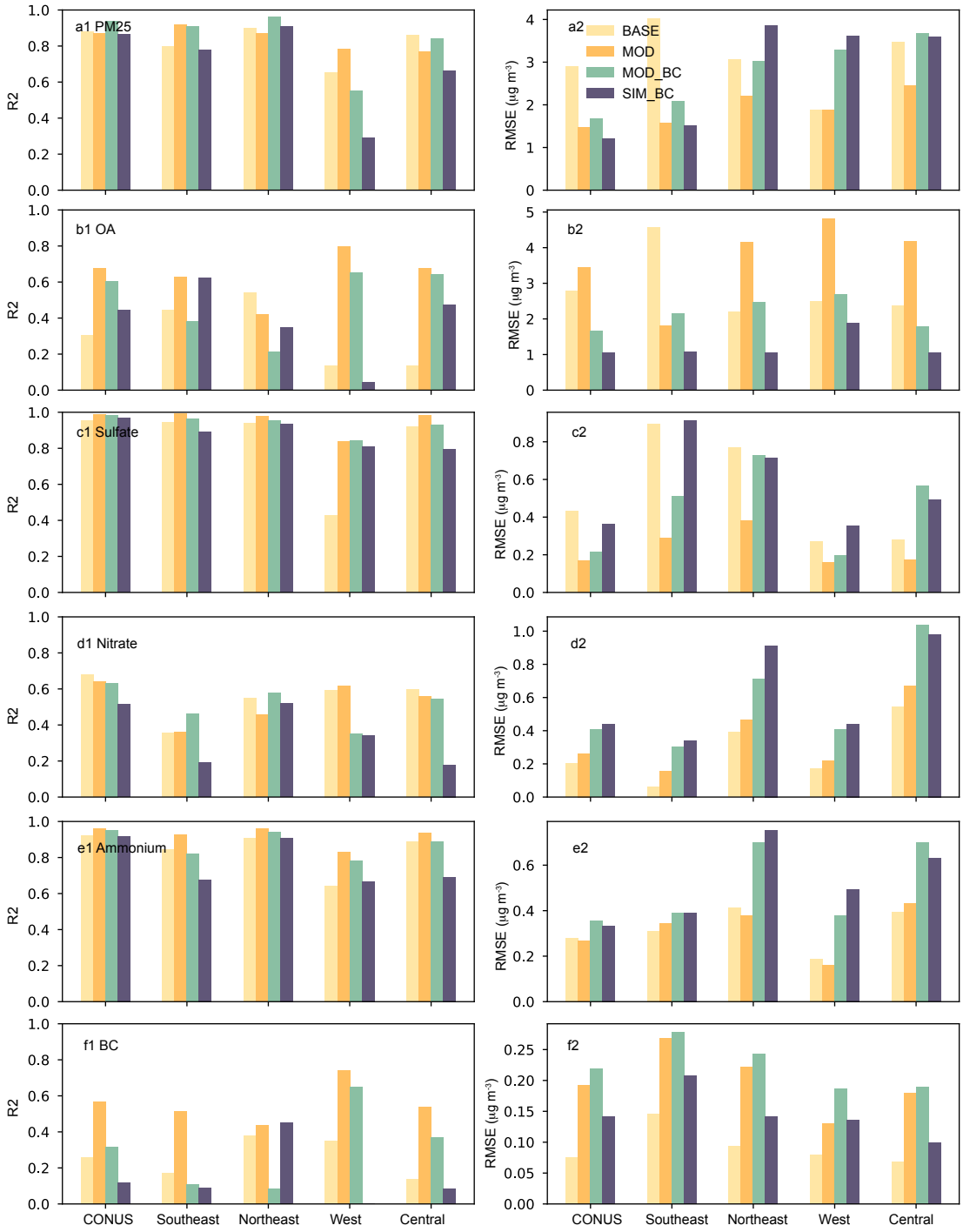

Supplementary Figure 11. Coefficient of determination (r^2) and root-mean-square error (RMSE) between observations and four GEOS-Chem cases for concentration of $PM_{2.5}$ and its five major components. Panels (a1–f1) show the r^2 values for $PM_{2.5}$, organic aerosols (OA), sulfate, ammonium, nitrate, and black carbon (BC), respectively. Panels (a1–f1) show the corresponding RMSE values for the same species.

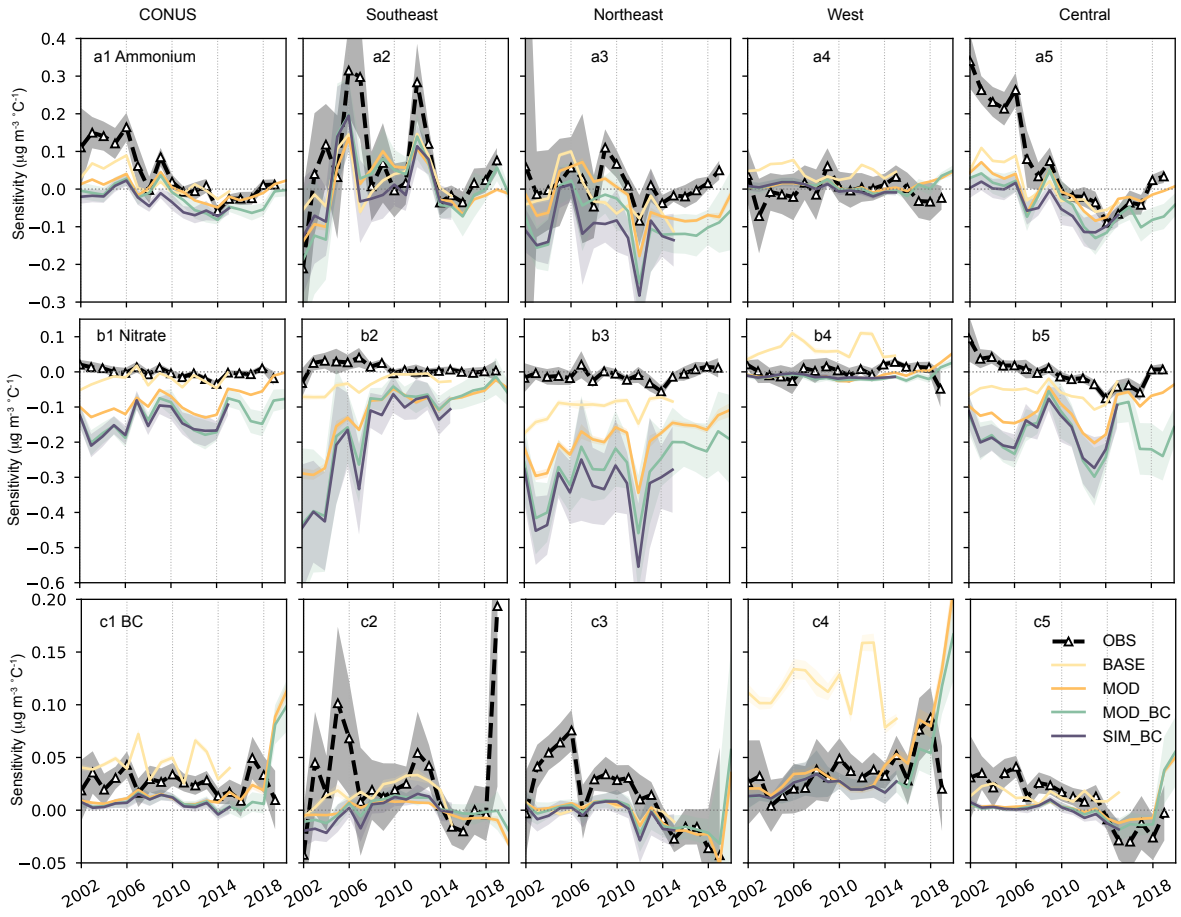

Supplementary Figure 12. Same as Figure 2 in the main text, but for ammonium, nitrate, and black carbon (BC).

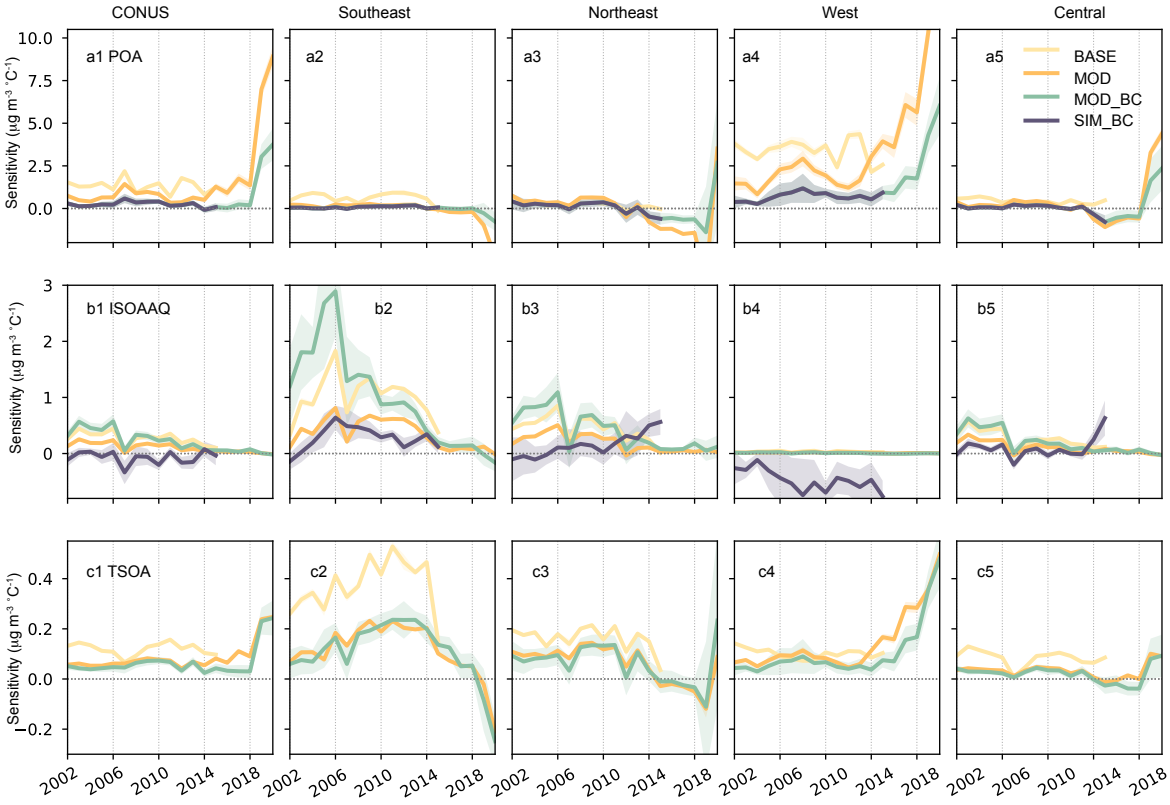

Supplementary Figure 13. Regional-aggregated temperature sensitivity of three major organic aerosol (OA) species from four GEOS-Chem cases. Panels a1-a5 shows the temperature sensitivity of primary OA for the contiguous US (a1), the Southeast US (a2), the Northeast US (a3), the West US (a4), and the Central US (a5); Panels b1-b5 shows the temperature sensitivity of aqueous-phase formed isoprene OA (ISOAAQ) for each region; Panels c1-c5 shows the temperature sensitivity of monoterpene SOA (TSOA) for each region. The SIM_BC case reports total SOA concentrations as a single variable SOAS, which is shown with ISOAAQ in panels b1-b5.

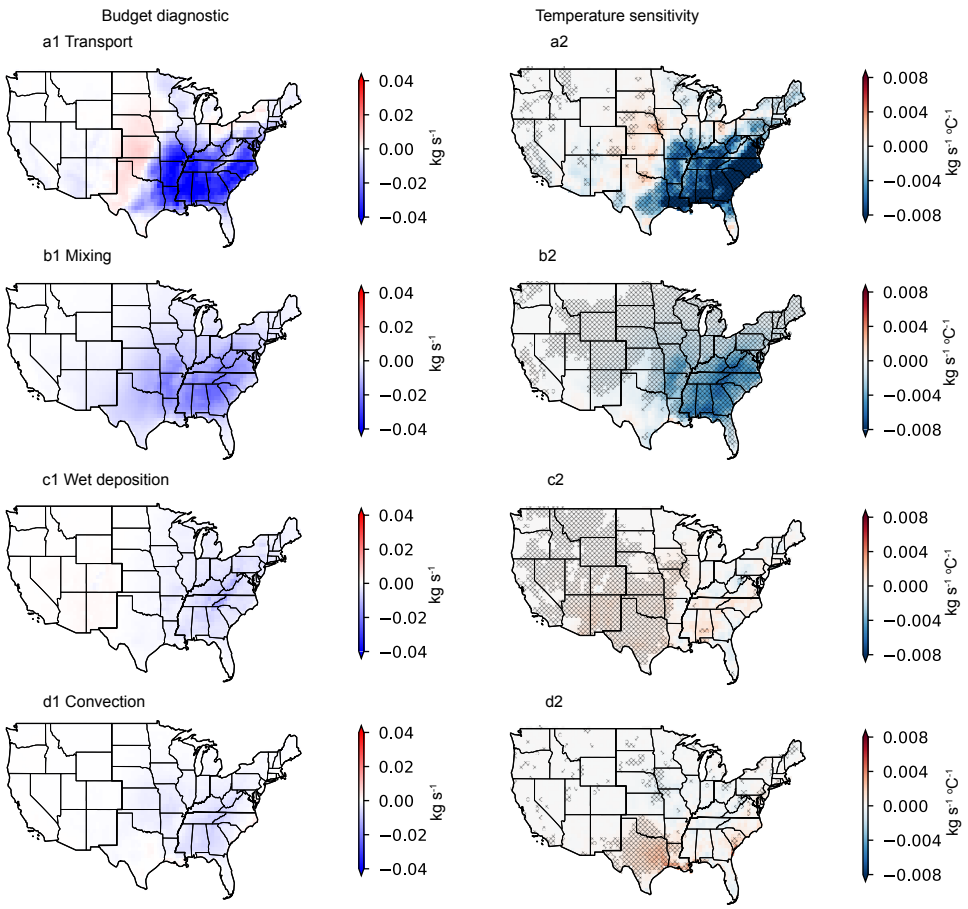

Supplementary Figure 14. Budget diagnostic for aqueous-phase-formed isoprene SOA (ISOAAQ) simulated by the MOD case and the temperature sensitivity of each process. Panels (a1–d1) show the budget diagnostic for transport (a1), mixing (b1), wet deposition (c1), and convention (d1) process and the corresponding temperature sensitivity (a2-d2).

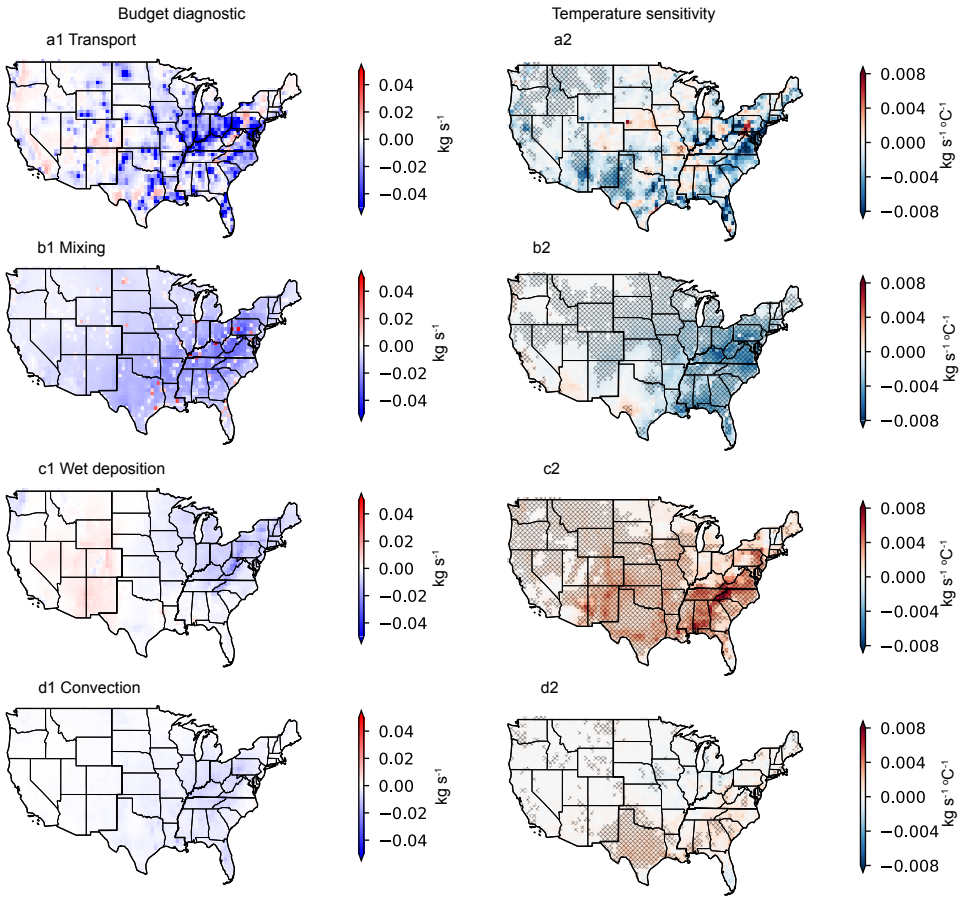

Supplementary Figure 15. Same as Supplementary Figure 14 but for sulfate budget diagnostic.

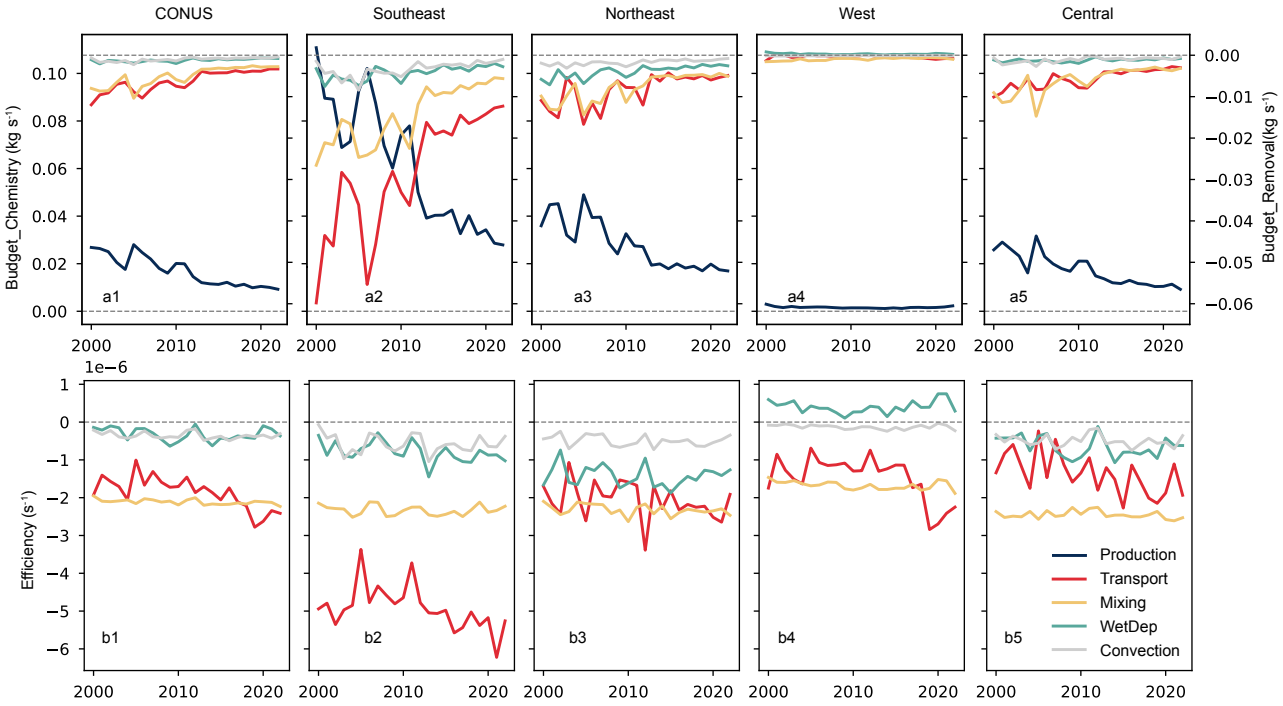

Supplementary Figure 16. Time series for budget diagnostic and efficiency of driving processes of ISOAAQ concentration. Panels a1-a5 shows the time series for budget diagnostic for the contiguous US (a1), the Southeast US (a2), the Northeast US (a3), the West US (a4), and the Central US (a5); Panels b1-b5 shows the time series for removal efficiency for each region.

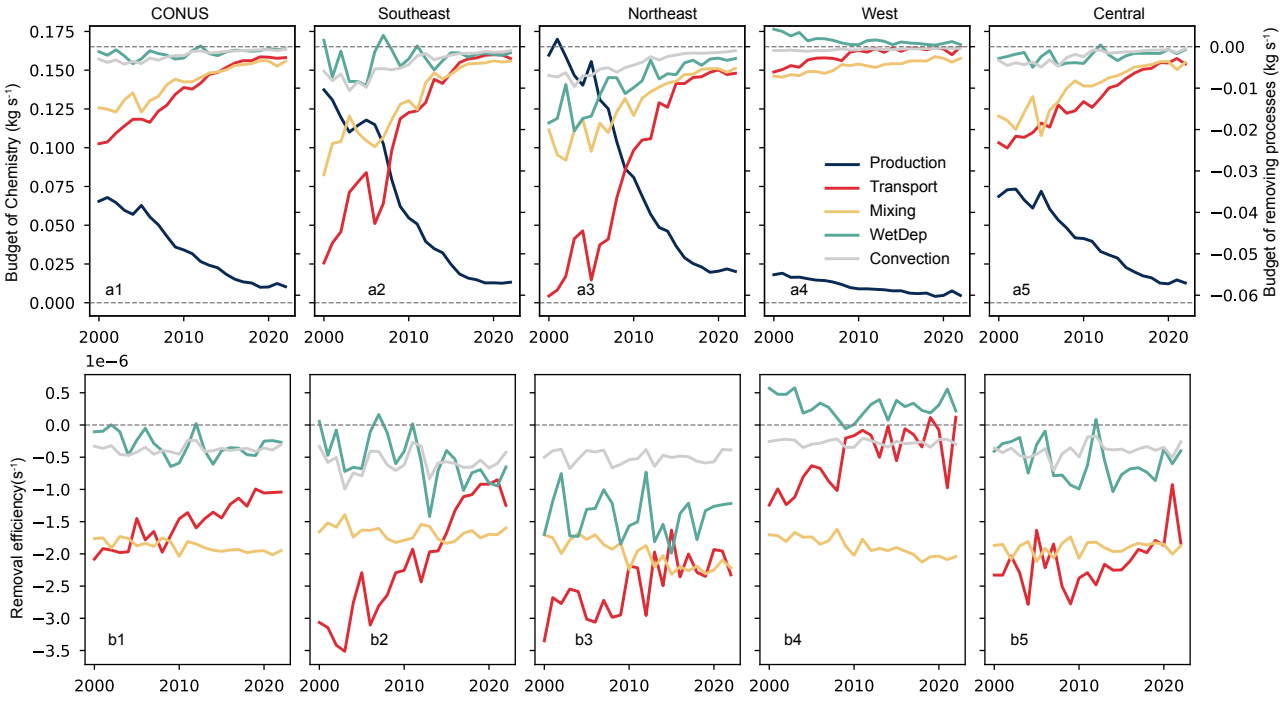

Supplementary Figure 17. Same as Figure 16 but for sulfate budget diagnostic.

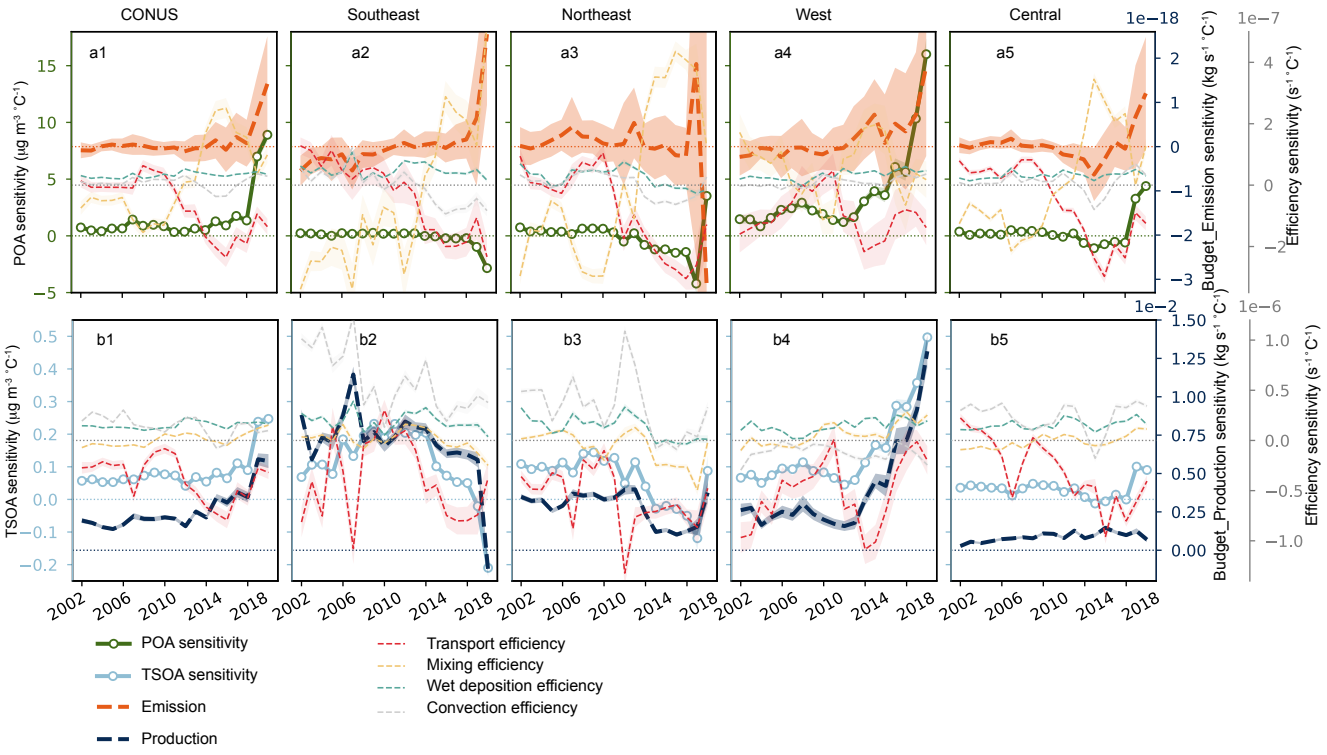

Supplementary Figure 18. Same as Figure 5 in the main text but for primary organic aerosol (POA) and secondary organic aerosol formed from monoterpene oxidation (TSOA).

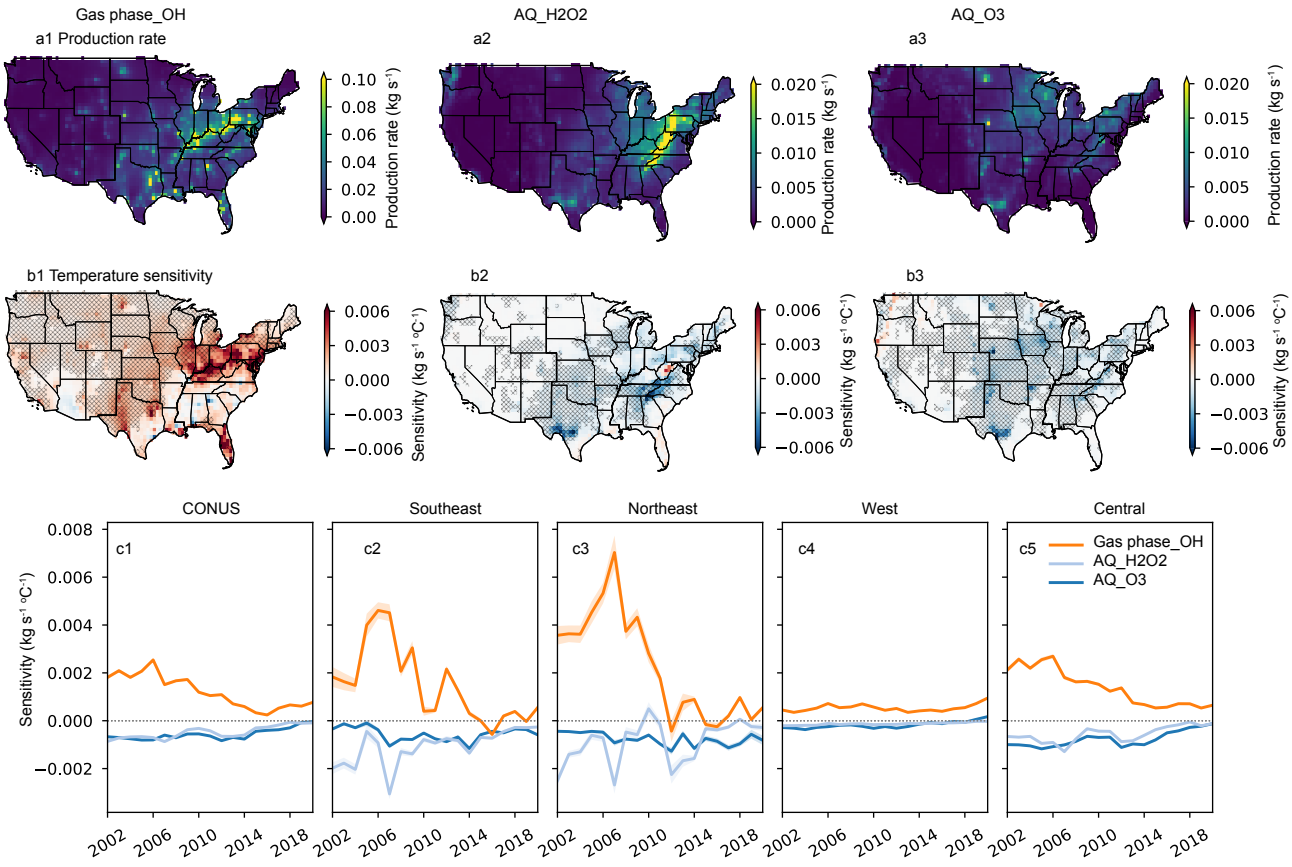

Supplementary Figure 19. Production rate (a1-a3) and corresponding temperature sensitivity (b1-b3) of three major sulfate production processes. Panels c1-c5 shows the time series for temperature sensitivity of each pathway for the contiguous US (a1), the Southeast US (a2), the Northeast US (a3), the West US (a4), and the Central US (a5).

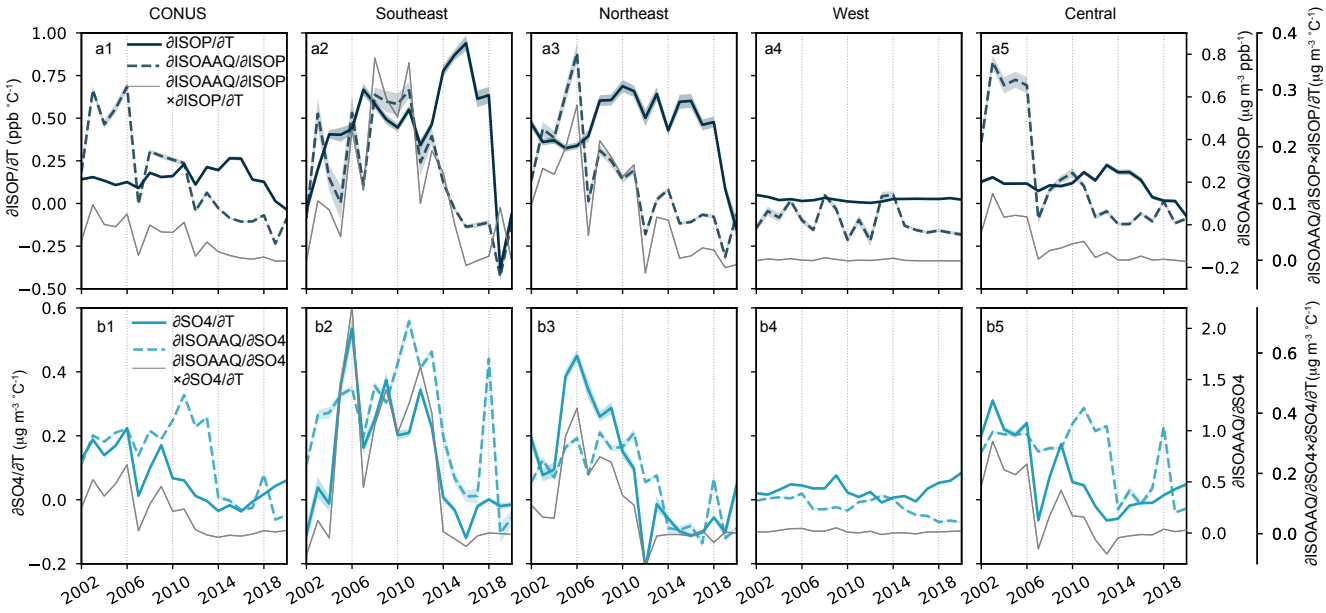

Supplementary Figure 20. Contributions from isoprene-mediated and sulfate-mediated processes to the overall temperature sensitivity of isoprene SOA (ISOAAQ). The shading areas represent 95% confidence interval. Panels a1-a5 show the time series of isoprene-mediated process breakdown for the contiguous US (a1), Southeast US (a2), Northeast US (a3), West US (a4), and Central US (a5); Panels b1-b5 show the time series of sulfate-mediated process breakdown for each region. Please refer to Eq. (1) in the main text for detailed expression.

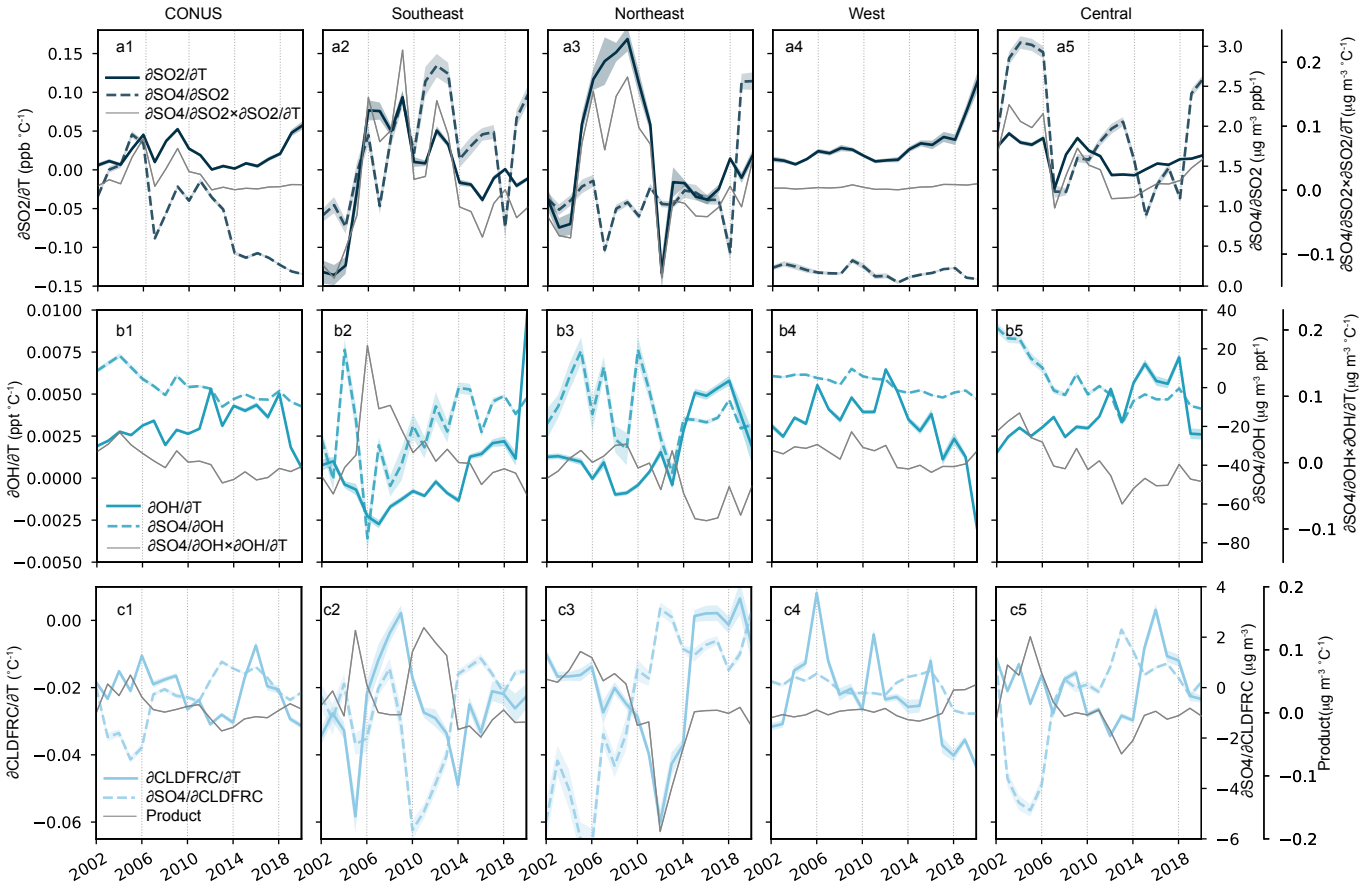

Supplementary Figure 21. Same as Supplementary Figure 20 but for sulfate. Please refer to Eq. (2) in the main text for detailed expression.

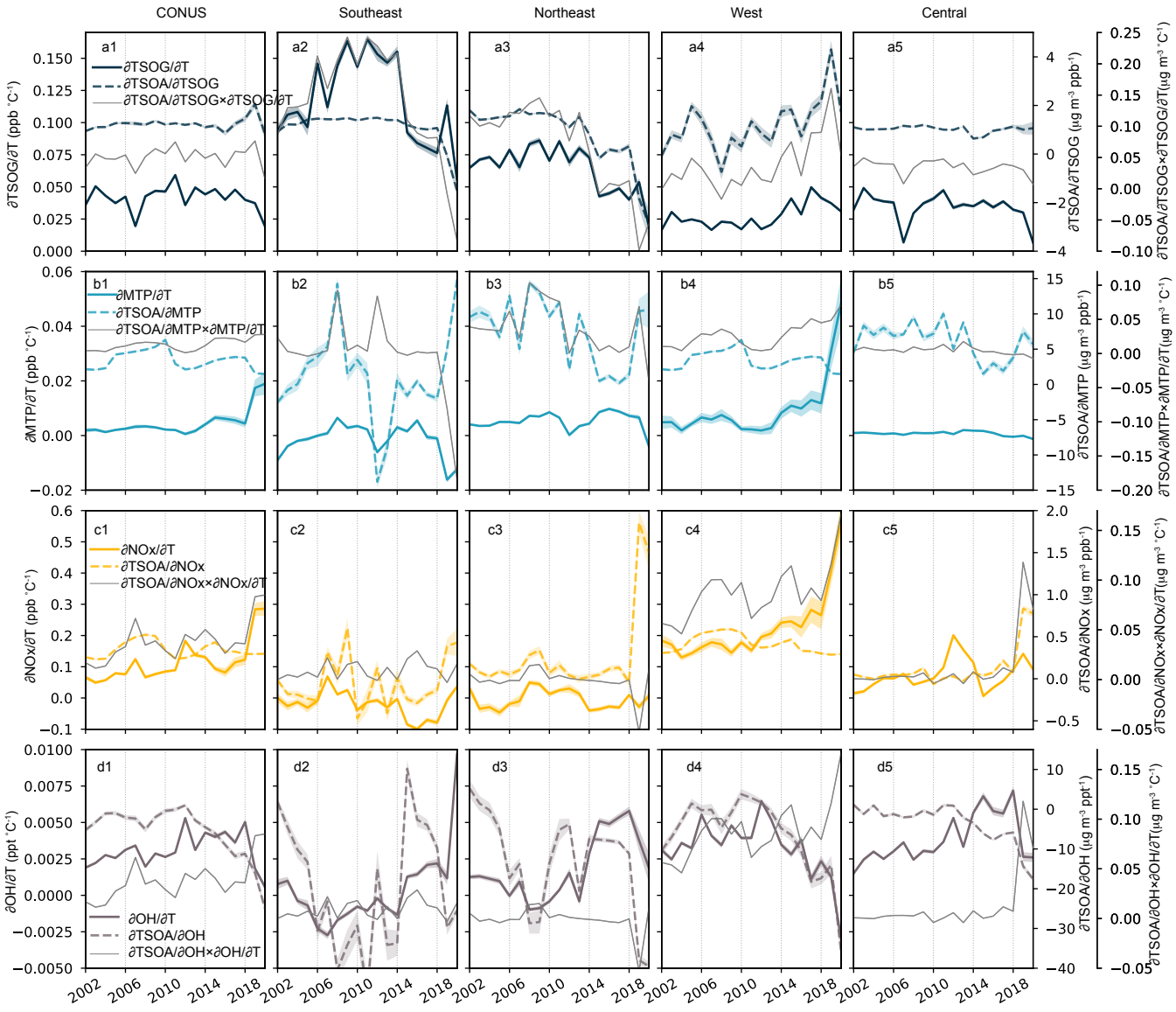

Supplementary Figure 22. Same as Supplementary Figure 17 but for monoterpene SOA (TSOA). Please refer to Eq. (3) in the main text for detailed expression.